A Rational Strategy for Reducing on-Target off-Tumor Effects of CD38-Chimeric Antigen Receptors by Affinity Optimization

Esther Drent[1], Maria Themeli[1], Renée Poels[1], Regina de Jong-Korlaar[1], Huipin Yuan[2], Joost de Bruijn[2,3], Anton C.M. Martens[1], Sonja Zweegman[1], Niels W.C.J. van de Donk[1], Richard W.J. Groen[1], Henk M. Lokhorst[1], Tuna Mutis[1]

[1]Department of Hematology, VU University Medical Center, De Boelelaan 1117, 1081HV Amsterdam, The Netherlands. [2]Xpand Biotechnology BV, Professor Bronkhorstlaan 10, 3723MB, Bilthoven, The Netherlands. [3]The School of Engineering and Materials Science, Queen Mary University of London, Mile End Rd, London E1 4NS, United Kingdom.

Amsterdam, North-Holland, The Netherlands

Correspondence should be addressed to T.M., t.mutis@vumc.nl
VU University Medical Center
Dept. of Hematology, CCA 4.22,
De Boelelaan 1117, 1081 HV,
Amsterdam, The Netherlands. Tel:+31(0)204447413

Short title: affinity-optimized CD38-CAR T cells

Abstract

Chimeric antigen receptors (CARs) can effectively redirect cytotoxic T cells toward highly expressed surface antigens on tumor cells. The low expression of several tumor-associated antigens (TAA) on normal tissues, however, hinders their safe targeting by CAR T cells due to on-target/off-tumor effects. Using the Multiple Myeloma (MM)-associated CD38 antigen as a model-system, we here present a rational approach for effective and tumor-selective targeting of such TAAs. Using the "light chain exchange" technology, we combined the heavy chains of two high-affinity CD38 antibodies with 176 germline light chains and generated ~124 new antibodies with 10 to >1000-fold lower affinities to CD38. After categorizing them in three distinct affinity classes, we incorporated the single-chain variable fragments of eight antibodies from each class into new CARs. T cells carrying these CD38-CARs were extensively evaluated for their on-tumor/off-tumor cytotoxicity as well as CD38-dependent proliferation and cytokine production. We identified CD38-CAR T cells of ~1000-fold reduced affinity which optimally proliferated, produced Th1 like cytokines and effectively lysed $CD38^{++}$ MM cells but spared $CD38^{+}$ healthy hematopoietic cells, *in vitro* and *in vivo*. Thus, this systematic approach is highly suitable for the generation of optimal CARs for effective and selective targeting of TAAs.

Introduction

Cytotoxic T cells endowed with chimeric antigen receptors (CARs) against surface antigens on tumor cells can induce powerful anti-tumor effects in experimental models and long term remissions in clinical trials. Specifically CAR T cells targeting CD19, an antigen present in B-cell leukemias and lymphomas, have shown impressive clinical results.[1–5] Hence, CAR T cells are currently considered highly appealing tools for cancer immunotherapy. Ideally the target molecule for CAR T cell therapy should be specifically expressed on tumor cells. Nonetheless, several years of research have identified only a few true tumor-specific surface antigens. Currently most tumor-associated target antigens (TAA) are expressed, albeit at low-to-intermediate levels, also on one or more normal tissues, such as epidermal growth factor receptors (EGFR and ErbB2/Her2), prostate specific membrane antigen (PSMA) or Carcinoembryonic antigen (CEA).[6,7] Targeting such antigens with CAR T cells raises safety concerns, due to on-target off-tumor toxicities with unpredictable severity. The application of carbonic anhydrase IX–specific CAR T cells in renal cell cancer resulted in liver toxicities[8] and CEA-specific CAR T cells in colon cancer patients induced severe colitis.[9] Additionally, a high antigen load, on tumor and healthy tissues can elicit a significant cytokine response when targeted with highly reactive T cells.[3,10,11] Targeting HER2 with CAR T cells caused a fatal cytokine release syndrome (CRS), due to the recognition of low levels of HER2 expressed on the cells of lung epithelium.[12]

In a recent preclinical study we have shown that CD38 is a useful target antigen for the treatment of multiple myeloma (MM) and that high affinity CD38-CAR T cells have significant anti-MM function *in vitro* and *in vivo*.[13] Although CD38 is expressed at very high levels on all MM cells, it is also present at intermediate levels on several hematopoietic cells, including NK cells, monocytes and a fraction of T cells. As expected, with high affinity CD38-CAR T cells we not only observed strong anti-MM effects, but also noted on-target off-tumor effects against normal hematopoietic cells.

Optimization of the design of the extracellular recognition domain of CARs has been proposed, among others, as an approach in order to enhance the capacity of CAR T cells to discriminate between tumors and normal tissues that express the same antigen in lower levels. Tumor selective effects of CARs

have been observed when using single chain variable regions (scFv) of existing low(er) affinity antibodies.[14–16] Thus, actively decreasing and optimizing the affinity of existing antibodies could allow for minimizing the off-tumor CAR responses, which in fact has been achieved by the introduction of mutations or the replacement of human with murine residues in the scFv domain.[16–19] Nonetheless, a convenient approach that can be utilized to *de novo* generation of a large panel of candidate scFvs and methodically selection of those CARs with an optimal target affinity is still lacking.

We here describe a rational and feasible strategy, using CD38 as a model-antigen, for tumor-associated but not entirely tumor-specific antigens. To generate new antibodies binding the same epitope with a broad range of different affinities, we used the light chain exchange technology.[20–23] Combining the heavy chains of two high-affinity CD38 antibodies with 176 germline light chains allowed the generation of more than a hundred new CD38 antibodies with 10-1000 fold lower affinities to CD38. The panel of candidate scFvs was narrowed down using rational selection criteria based on the desired immunotherapeutic properties of CAR T cells. Systematic *in vitro* and *in vivo* analysis of the newly generated CARs revealed that CAR T cells bearing scFvs derived from ±1000-fold lower affinity antibody were tumor selective killers with strong lysis of $CD38^{++}$ MM cells and little or no lysis of $CD38^{+}$ normal human hematopoietic cells.

Methods

Antibody production by Light chain exchange

Variable heavy- and light chain coding regions were cloned in the pcDNA3.3 (Invitrogen) based vectors p33G1f and p33Kappa respectively. All 352 antibodies were produced under serum-free conditions by individually co-transfecting 2 heavy chains (024 and 028) and 176 germline light chain expression vectors in HEK-293F cells, using 293fectin (Invitrogen), as previously described.[24] A simple, robust and highly efficient transient expression system for producing antibodies.[24] Cell-free supernatants were harvested and antibody concentrations were determined by Octet IgG quantification (Forté Bio).

Bio-layer interferometry

Affinities were measured and ranked using biolayer interferometry on a Octet HTX instrument (ForteBio). Anti-Human IgG Fc Capture biosensors (ForteBio) were loaded for 1000 s with hIgG1 containing different heavy and light chain combinations directed against CD38. After a baseline (100 s) the association (1000 s) and dissociation (1000 s) of the extracellular domain of N-terminally His-tagged CD38 (His-CD38,100 nM) in Sample Diluent (ForteBio) was determined. For calculations, the theoretical molecular mass of His-CD38 based on the amino acid sequence was used, i.e. 30.5 kDa. Experiments were carried out while shaking at 1000 rpm and at 30 °C. Data was analyzed with Data Analysis software v8.0 (ForteBio), using the 1:1 model and a local full fit with 1000 s association time and 250 s dissociation time. Data traces were corrected by subtraction of the average of 4 reference biosensors loaded with IgG1-3003-028 WT and incubated with Sample Diluent only. The Y-axis was aligned to the last 5 s of the baseline, and interstep correction as well as Savitzky-Golay filtering was applied.

Antibody Binding assay

Homogenous binding assays for human CD38 specific antibodies were performed in 1536 well microtiter plates in dose response using a Tecan Evo 200 liquid handler. Binding of IgG1 antibodies to

CHO cells transiently expressing human CD38, CHO wt background control and streptavidin beads coated with purified biotinylated his-tagged human CD38 was detected with a secondary polyclonal goat IgG anti-Human IgG (Fc) - Alexa Fluor 647 conjugate (Jackson ImmunoResearch). In parallel, the binding of IgG1 antibodies to streptavidin beads coated with purified biotinylated his-tagged human CD38 was also assessed using a monovalent secondary goat Fab anti-Human IgG, (H+L) - DyLight 649 conjugate (Jackson ImmunoResearch). IgG1 samples were normalized and diluted in Freestyle 293 expression medium (Gibco). Two microliter of diluted sample was added to 5 microliter cell or bead suspensions containing secondary conjugates at 200 ng/mL IgG conjugate or 300 ng/mL Fab conjugate, respectively. Cell suspensions were prepared in FMAT buffer (PBS, 0.1% BSA and 0.02% Sodium Azide) + 0.075% Pluronic F-68. Bead suspensions were prepared in HBB (10-mM HEPES (pH 7.4), 150 mM NaCl, 5 mM KCl, 1 mM MgCl2, 1.8 mM CaCl2, 0.5% BSA and 0.01% Sodium Azide + 0.075% Pluronic F-68). After 8 hours incubation at RT in the dark, fluorescence signals were recorded using the Applied Biosystems 8200 Cellular Detection System (ThermoFisher Scientific) with a 50 counts cut-off value applied. Obtained total fluorescence intensity data was processed and visualized using ActivityBase software (IDBS).

Introduction of CD38-specific scFvs in CAR constructs

The selected variable light and heavy chains were amplified using PCR with primers (supplemental table S3) containing homology arms and Gibson assembly (NEB) was used to combine both chains linked with a G_4S linker. The generated scFvs were cloned into SFG retroviral vector, followed by a CD8a transmembrane domain and the 4-1BB and CD3ζ signaling domains as described in Zhao et al.[25] The CAR constructs were linked by a 2A sequence to a truncated NGFR or dsRed sequence.[26]

Generation of retroviral particles and transduction of T cells

Phoenix-Ampho packaging cells were transfected with the CAR constructs, gag-pol (pHIT60), and envelope (pCOLT-GALV) vectors (Roche). Two and three days after transfection, cell free supernatants containing retroviral particles were collected and directly used for transduction.

Peripheral Blood Mononuclear cells (PBMCs) from healthy donors were stimulated with lectin-like phytohemagglutinin (PHA-L) in RPMI-1640 + 10% FBS. After 48 hours, cells were retrovirally transduced using spinoculation on retronectin (Takara) coated plates in the presence of Polybrene .A second transduction was done after 16 hours. 72 hours post-transduction LNGFR or dsRed and CD38 expression was determined by flow cytometry. T cells were expanded using culture medium (RPMI-1640, 10% human serum, antibiotics), and 50 IU/ml rhIL-2 (Proleukin®, Novartis). One week after, CAR-transduced T cells were either stimulated with irradiated (5 Gy) UM9 cells (E:T ratio 1:3) or tested functionally.

Primary cells from MM patients and healthy individuals.

Bone marrow mononuclear cells (BMMC) containing 5-40% malignant plasma cells were isolated from bone marrow aspirates of MM patients through Ficoll-Paque density centrifugation and either used directly or cryopreserved in liquid nitrogen until use. PBMCs/MNCs were isolated from Buffy coats of healthy blood-bank donors by Ficoll-Paque density centrifugation. All primary samples were obtained after informed consent and approval by the institutional medical ethical committee.

Cell lines

Unmodified or luciferase (Luc-GFP)-transduced human MM cell lines, UM9 and RPMI8226 were cultured in RPMI-1640 (Invitrogen) + 10% FBS (Invitrogen) + antibiotics (penicillin;10.000 U/ml, streptomycin; 10,000 µg/ml) as described.[13]

Cloning, expression and purification of CD38 extracellular domain (sCD38)

A synthetic DNA construct encoding the Honeybee Melittin signal sequence (HMSS) fused to a fragment of the extracellular CD38 domain encoding residues 43-400 was purchased (GeneArt). The HMSS-CD38 DNA was cloned into the pFastBacNKI-LIC-3C-his vector[27] to get pFastBACNKI-HMSS-CD38-3C-his (C-terminal 6xhis-tag). Bacmid DNA and virus were essentially prepared according to the Bac-to-Bac manual (Thermo Fisher Scientific). Briefly, the pFastBACNKI-HMSS-CD38-3C-his construct was transformed into EMBACY cells[28] and bacmid DNA was isolated. Sf9

insect cells were transfected with bacmid DNA and virus was harvested. Virus was amplified and used to infect sf9 cells for protein expression. Secreted proteins were harvested and concentrated in using a Fresenius Polysulfone F40S dialyzer (Fresenius Medical Care). CD38 was purified on a HiTrap Ni2+ column and eluted with 200 mM imidazol in 25 mM NaCl pH 8.0, 200 mM NaCl. CD38 was further purified by size exclusion chromatography on a S200 16/60 Superdex column (GE Healthcare) equilibrated with 25 mM NaCl pH 8.0, 200 mM NaCl buffer. The protein eluted in a single peak and fractions containing the protein were pooled and concentrated.

Flow cytometry

Flow cytometry assays were performed on FACS CantoII or LSR Fortessa (BD). Different cell subsets in T cells, PBMC or in BM-MNC in were determined using fluorescein conjugated antibodies specific for human CD3, CD4, CCR7, CD8, CD14, CD19, CD38, CD45, CD45RA, CD56, CD62L, and CD138 (BD Bioscience). Viable cells were determined with live/dead cell marker (LIVE/DEAD® Fixable Near-IR; Life Technologies L10119).

Detection of CAR expression

The sCD38 protein was used in flow cytometry experiments to determine the cell surface expression levels of high affinity CARs and to correlate to this with the expression of LNGFR, measured with an either PE or APC conjugated antibody to LNGFR (CD271) (Biolegend).An almost perfect correlation was found between the sCD38-aided measurement of CAR expression and the NGFR expression (supplemental Fig. S2). After this validation, transduction efficiency and associated CAR expression of other CAR transduced cells was done by NGFR measurements since sCD38 did not bind to CARs with low affinity. We confirmed a comparable NGFR expression in all tested CAR T cells, the expression of the selected CARs are depicted in supplemental Fig. S3.

Flow cytometry-based cytotoxicity assay

Seven to ten days after transduction serial dilutions of CAR T cells were incubated with Violet tracer (Thermo Fisher) labeled BM-MNC or PBMC for 6-24 hours. After addition of Flow-Count™

Fluorospheres (Beckman 7547053) cells were harvested and stained for different CD markers (see above). Viable cells were then quantitatively analyzed through Flow-Count-equalized measurements. Percentage cell lysis was calculated as followed and only if the analyzed target cell population contained >500 viable cells in the untreated samples. % lysis cells = 1 − (absolute number of viable target cells in treated wells / absolute number of viable target cells in untreated wells) × 100%.

Bioluminescent Imaging based cytotoxicity assay

To determine the lysis of Luc-GFP-transduced human malignant cell lines by CD38-CAR T cells seven to ten days after transduction., Serial dilutions of mock or CD38-CAR T cells were co-incubated with the malignant cell lines. The luciferase signal produced by surviving malignant cells was determined after 16-24 hours with a GloMax® 96 Microplate Luminometer (Promega) within 15 minutes after the addition of 125 µg/mL beetle luciferin (Promega). % lysis cells = 1 − (BLI signal in treated wells / BLI signal in untreated wells) × 100%.

Cytokine measurement

To determine the broad array of cytokines produced by CAR T cells, we used the Cytokine Bead Array (CBA) Human Th1/Th2 cytokine kit (BD) according to manufacturer protocol. In brief, CAR T cells at 7 days post transduction were stimulated with either UM9 or U266 cells for 24 hours. Cell free supernatants were harvested and incubated with a mixture of capture beads (IL-2, IL-4, IL-5, IL-10, TNF and IFN-γ), PE-detection reagent for 3 hours. Beads were washed and analyzed by a standardized flow cytometry assay.

Hematopoietic progenitor cell growth inhibition assay

A total of 1000 $CD34^+$ sorted BM cells were mixed with effector CART cells at a CART:BM cell ratio of 1:1 in 0.2 mL of RPMI culture medium. After culturing for 4 hours in this small volume, the cells were resuspended to a final volume of 2 mL with semisolid Methocult (Stem cell technologies, H4534),then plated in 6cm dishes and incubated at 37°C in 5% CO_2. After 14 days, the number of

colony-forming unit-granulocytes (CFU-G), and CFU-monocytes (CFU-M), were scored under a microscope.

***In vivo* xenograft studies**

RAG2$^{-/-}\gamma c^{-/-}$ mice used in this study were originally obtained from the Amsterdam Medical Center (AMC, Amsterdam, the Netherlands) and were bred and maintained at the Amsterdam Animal Research Center. All animal experiments were approved by local ethical committee for animal experimentation and were in compliance with the Dutch Animal Experimentation Act.

We used an *in vivo* model, in which a humanized bone marrow-like environment is created in mice[29]to allow the growth of human MM tumors or normal CD34$^+$ cells in their natural niche. Briefly, hybrid scaffolds consisting of three 2- to 3-mm^3 triphasic calcium phosphate particles were coated *in vitro* with human bone marrow mesenchymal stromal cells (BM-MSC)(2×10^5 cells/scaffold). The scaffolds were implanted subcutaneously into the mice[29]. Eight to twelve weeks after implantation, mice were i.v. injected with luciferase-transduced UM9 MM cells to monitor the anti-tumor effects of CAR T cells. In a separate experiment, fluorescent (FarRed) labeled CD34+ cells were injected into the scaffold to monitor the on-target off-tumor effect of CAR T cells. After one week, when the tumors or CD34$^+$ cells became detectable by bioluminescence imaging (BLI) or Fluorescence life imaging (FLI), respectively, mice were divided in equal groups; CD38-CAR- or mock-transduced T cells (5×10^6 cells/mice) were injected by tail i.v. injections. Tumor growth or CD34$^+$ cell persistence was monitored by weekly BLI measurements. Postmortem bone marrow, spleen and scaffolds were harvested from each mouse, dissociated (spleen and scaffolds), filtered through a 70 μm filter and single cell suspensions were counted, stained and measured by flow cytometry.

Statistical methods. Statistical analyses were performed using Graphpad Prism software 6. In analyses where multiple groups were compared, either a parametric ANOVA or nonparametric Kruskal-Wallis test were used with subsequent multiple comparison. A p value <0.05 was considered significant.

Results

Generation of lower affinity CD38 antibodies by light chain exchange.

To generate lower affinity CD38 antibodies we applied the light chain exchange technology, in which we combined the heavy chains of high affinity antibodies 028 and 024 (described in patents WO2011154453 and WO2006099875) with 176 random germ line light chains, schematically depicted in figure 1A. One of these two antibodies, 028, was previously used to generate high affinity CD38-CAR T cells.[13] Based on previous studies, pairing of heavy chains with numerous different light chains (light chain exchange or light chain shuffling) results in the alteration of binding affinity but not epitope specificity of the antibody.[21,22,30–32] Among 352 combinations, 262 antibodies were properly expressed in sufficient quantities, and 124 of them showed binding towards $CD38^+$ transfected, but not $CD38^-$ WT CHO cells (Fig. 1B first and fourth panel) indicating their CD38 specificity. 69 of these 124 antibodies also showed binding to recombinant CD38 coated beads. While 23 of these 69 antibodies showed bivalent binding (IgG), the remaining 46 displayed bi- and monovalent (Fab fragment) binding (quantified EC50 values for each detection method are depicted in Fig. 1C). Antibodies with the strongest binding capacity also displayed a detectable biolayer interferometry signal on an Octet HTX instrument, whereby the on-rate (k_{on}), off-rate (k_{off}) and affinity constant (K_D) (Fig. 1D and E) could be determined. As illustrated in figure 1E left panel, the K_D values of those antibodies were 10 to 1000 times lower than the K_D of the original antibody 028. Based on these data we classified all functional antibodies into three classes: Class A represented antibodies with a similar binding profile to CD38 as the parental (wildtype) antibodies but with ±10-1000 x lower affinity. Class B antibodies had no detectable affinity by biolayer interferometry but binding to CD38-positive cells/beads, (thus >1000x lower affinity to the original antibody), while the class C antibodies showed solely binding to CD38 positive cells, thus with an affinity even lower than the category B. Sequence similarities and differences in complementary determining regions (CDRs) of these antibodies are illustrated in supplemental table S1. We selected 8 antibodies from each class and generated 24 different CARs using their scFvs. A selection of soluble scFvs were evaluated for unwanted, induced aggregation or impurity, to exclude protein instability as a cause for their altered affinity

(supplemental Fig. S1). PBMC-derived T cells from a healthy donor were transduced with the selected 24 newly generated CARs.

Anti-Myeloma activity of CD38-CAR T cells with variable affinities.

Since the anti-tumor function of CAR T cells is of primary importance, we first determined the lytic capacity of the newly generated CD38-CAR T cells against the CD38-positive MM cell line UM9. While CAR T cells generated from class C antibodies did not lyse the UM9 cells at all, T cells transduced with CARs from Class B and A antibodies were capable of lysing MM cells. As predicted, the highest affinity CARs (class A) were better in lysing tumor cells, compared to class B (Fig. 2). Interestingly, some T cells transduced with class A antibodies (CARAx T cells) lysed the UM9 cell line as effective as the CAR T cells which were generated from the original 028 antibody (CAR028 T cells) despite their much lower affinity for CD38. On the other hand, all CARs with the 024 variable heavy chain (VH) (CARs 5 - 8 in each class) elicited inferior tumor cytotoxicity compared to CARs generated using the VH of the 028 antibody (CARs 1 - 4 in each class). Based on these results, 2 of the best CARs from both class A and B were selected (CARA1, A4, B1 and B3) (Fig. 2 indicated with arrows), and were analyzed for their proliferative capacity cytokine production and on-target off-tumor cytotoxicity to gain more insight into their immunotherapeutic properties.

Cytokine release of lower affinity CAR T cells

The selected CAR T cells were first tested for their CD38-dependent cytokine production after stimulation with MM cell line UM9. All four CAR T cells, similar to the control high affinity CAR028 T cells, produced IFN-γ, IL-2 and TNFα in the presence but not in the absence of CD38+ target (Fig. 3A). Little or no IL-4, IL-5 or IL-10 (supplemental Fig. S4) were produced, thus indicating a typical Th1 cell phenotype. The level of cytokine production showed some association with the CAR affinity for CD38. Importantly however, the level of cytokine secretion by CARA1- and A4-transduced T cells showed no substantial difference from the high affinity CAR028 T cells.

Proliferation and expansion of lower affinity CAR T cells

We have previously showed that high affinity CD38-CAR T cells display a slower growth rate in the first two weeks due to fratricide. After this period they readily expanded, but displayed no CD38 expression on the cell surface. Therefore we also tested the CD38-dependent *in vitro* proliferative capacity and the immunophenotype of the four candidate CAR T cells after one week of transduction and after weekly stimulations with irradiated UM9 cells (Fig. 3 B and C indicated with arrows). The candidate CAR T cells displayed a similar or better growth rate compared to the control CAR028 T cells with the exception of CARA1 T cells. Furthermore the CARA4-, B3- and B1-T cells retained their CD38 expression, as opposed to CAR028 T and CARA1 T cells, (supplemental Fig. S3 right panel). Interestingly, lower affinity CAR T cells contained >50% central memory cells at the end of the production stage (1 week after transduction), similar to the mock control and in contrast to CAR028 T cells. As expected, however all cultures converted to predominantly effector memory (EM) cells after *in vitro* stimulation and expansion with tumor cells (Fig. 3C).

T cells endowed with lower affinity CARs mediate no or minimal off-tumor effects

Since our specific aim was to generate CAR T cells with minimal off-tumor on-target effects by affinity optimization, we finally determined the cytotoxic activity of the four selected CARs towards MM cells as well as normal healthy cells. Although CD38 can be expressed on several tissues, we studied hematopoietic cells as the prominent candidates of off-tumor effects because preliminary immunohistochemistry assays of several normal tissues revealed that the expression of CD38 was the highest in hematopoietic cells (data not shown). For a side-by-side comparison of the on-tumor and off-tumor effects, we used primary bone marrow mononuclear cells (BM-MNCs) from MM patients as target cells, in which $CD38^{+}$ normal hematopoietic cells coexist with $CD38^{++}$ primary MM cells. Thus, after incubation of CAR T cells with BM-MNC we determined the lysis of MM cells and normal hematopoietic cells in the same sample by quantitative flow cytometry. The CAR T cells lysed $CD38^{++}$ MM cells in a roughly affinity-associated fashion ranging from 98% lysis for CARA1 to 68% lysis for the lowest affinity CARB3. (Fig. 4A top panel). Importantly, the lysis levels of CARA1 and CARA4 T cells did not significantly differ from the control CAR028 T cells

The lysis of $CD38^+$ fractions of normal B, T, NK cells and monocytes by CARA1, A4, B1 and B3 T cells comprised 84, 24, 23 and 6%, respectively, while the mock T cell mediated background lysis was 7%. Thus except CARA1 T cells, all other candidates showed negligible or no off-target effects on $CD38^+$ fractions of normal hematopoietic cells. When the hematopoietic cells were analyzed regardless of CD38 expression the total hematotoxicity of CARA1, A4, B1 and B3 T cells comprised only 20, 3, 20, 0%, respectively of which 11% was background, mock T cell mediated lysis. In contrast, the off-tumor effect of control CAR028 T cells was substantially higher (90% lysis of $CD38^+$ fraction; 39% lysis regardless of CD38 expression) (Fig. 4 B, C, illustrative flow cytometry plots in 4D). These data indicate that indeed the newly generated low affinity CAR T cells have minimal off-tumor effects.

Selection of the best lower affinity CD38-CAR T cells.

Finally, to rationally select the most optimal CAR T cell, we summarized the *in vitro* data of the candidate CD38-CAR T cells, primarily according their anti-MM cytotoxicity and off-tumor hematopoietic cell toxicity, and secondarily according to cytokine production and proliferative capacity (supplemental table S2). Based on these criteria we excluded CARB3 T cells due to too low anti-tumor reactivity and CARA1 T cells due to too high off-tumor effects (Fig. 5). The remaining candidates were compared according to the secondary criteria. The CARA4 appeared the best performer since its proliferative capacity and especially the cytokine production was much better than that of CARB1.

The *in vivo* anti-tumor effects of CARA4 T cells

We then evaluated the *in vivo* anti-tumor and off-tumor effects of CARA4 T cells and compared these effects with those of CAR028 and mock T cells. To mimic the human MM microenvironment, we used the specific $Rag2^{-/-}\gamma c^{-/-}$ xenograft murine model, where the luciferase transduced tumor cells are grown in humanized BM like-niches generated by subcutaneous implantation of ceramic scaffolds coated with human bone marrow stromal cells (hu-BMSCs).[29] As illustrated in figure 6A, in the negative control group treated with mock T cells, tumors showed a fast progression. Although not

curative, treatment of the tumor-bearing mice either with CAR028 or CARA4 T cells induced a significant and apparently similar anti-tumor effect (Fig. 6A, B). We did not encounter a tumor escape due to antigen-loss variants since post mortem analyses revealed that all remaining tumor cells in the mice were $CD38^+$ (supplemental Fig. S6).

The *in vivo* on target off-tumor effects of CARA4 T cells

In the *in vivo* model we observed the maximum anti-tumor effects in the first three weeks (Fig. 6). To evaluate whether the CARA4 T cells or CAR028 T cells would induce any undesired on-target off-tumor effects in this period, we injected fluorescent (FarRed) labeled $CD38^+CD34^+$ normal hematopoietic progenitor cells in the humanized scaffolds and treated the mice with i.v. injected CAR T cells. The FLI signal from normal hematopoietic progenitors was followed during 3 weeks. Injection of CARA4 T, CAR028 T or mock T cells had no effect on the FLI signal (Fig. 7A). This observation was confirmed by CAR028 and CARA4 pre-treated CD34 cells, which could still form similar numbers of colonies in a colony forming assay (supplemental Fig. S7). Nonetheless, post-mortem analysis, after three weeks revealed in mice treated with CAR028 T cells significantly lower percentages (Fig. 7B) and total cell numbers (Fig. 7C) of $CD38^+$ cells within the $CD34^+$ fraction. Similar results were observed within the more differentiated $CD34^-$ fractions as compared to CARA4 T cell treated animals (Fig. 7B and C).

This indicated that CARA4 had no effect on $CD34^+$ progenitor cells or more differentiated hematopoietic cells even if they expressed CD38. In contrast, treatment with CAR028 T cells did not hamper the total FLI signal, mediated toxicity against all $CD38^+$ cells including the progenitor and differentiated cells. Since this could eventually result in defects in the differentiation of some lineages we concluded that CARA4 cells were also better performers *in vivo*.

Discussion

CAR T cells have produced remarkable clinical results when targeting CD19, a surface molecule present on B-cell malignancies.[33] However, the broader application of CAR T cell therapy on the majority of cancers is limited by the simultaneous expression of TAAs - which are otherwise attractive CAR targets - on healthy tissues. Here, we propose a new feasible technique for the generation of a large panel of antibodies with different affinities. A systematic analysis and careful identification of suitable scFvs, enabled CARs that effectively target tumors with little or no off-tumor effect. We show that TAAs, such as CD38 for MM, can be selectively targeted by an scFv with an optimal affinity to the target antigen.

Equipping CARs with scFvs of lower affinity has been shown to avert on-target off-tumor effects and create a tumor selective window for targeting TAA with CAR T cells.[14,15] Tuning the affinity of existing antibodies by single amino acid substitutions in the scFv region[16,18] can be a useful method to create a panel of alternative CAR constructs. However, the optimal affinity range appears to differ enormously when targeting different epitopes or target antigens. Chmielewski *et al*[18] described affinities of 15-16 nM as optimal for tumor-selective ErbB2 targeting whereas Liu et al. determine an optimal antibody affinity of 1.1 nM for the same antigen. In our study, we exchanged the antibody light chain while keeping the heavy chain constant, which is suggested to modulate the affinity but not the epitope specificity of an antibody.[30,31] In contrast to previous studies, in which a limited panel of no more than 8 new scFvs was tested,[15,16,19,34] the light chain exchange technology allowed us to rapidly generate hundreds of new antibodies with a large range of affinities to the CD38 molecule. Thus, we were able to methodically identify the optimal candidate with the desired immunotherapeutic properties whereby a truly tumor-selective cytotoxic activity could be achieved. In fact our results as well as the results of others,[14–16,34] indicate that such a systematic approach is necessary because, as mentioned above, there are yet no universal parameters, which could help to predict the optimal antibody/scFv affinity for each epitope and every target antigen. Interestingly, with this technique we could lower the highest antibody affinity of 1.8 nM more than a 1000-fold and still obtain CARs with significant anti-tumor cytotoxicity and minimal off-tumor effects. While we have not tested the

affinity of the scFvs to the CD38 antigen, the affinities of the selected antibodies correlated well with the CAR activity.

In order to select the optimal CAR construct we followed a logical approach in which we started with heavy chains of two high affinity antibodies (024 and 028) and extensively characterized the generated new antibodies for their affinity. We then categorized these antibodies into three "affinity groups" and selected 8 representative antibodies from each group, hereby pragmatically decreasing the pool to 24 scFv candidates to construct new CARs. The resulting 24 CAR constructs were first screened according to their anti-tumor cytotoxicity, since this is the most crucial desirable immunotherapeutic function. This approach appeared highly convenient since we could readily eliminate all antibodies within the lowest affinity class. Furthermore, although the candidate antibodies did not show significant affinity differences, the CARs generated from the 024 heavy chain were in general inferior as compared to CARs generated from 028 heavy chain, indicating the importance to start with more than one heavy chain, whenever possible. Although some 024 CARs showed intermediate lysis of MM cells, we continued only with 028-antibody based CARs, as there were already excellent candidates within this category. We extensively evaluated 4 candidates from this group which elicited >50% anti-tumor cytotoxicity in our *in vitro* assays. To select the most optimal CAR we thoroughly evaluated their several functional properties such as cytokine secretion, long-term antigen-specific proliferation, immunophenotype, but more importantly their on-target and off-tumor cytotoxicity against primary human samples. We finally selected the CARA4 as the most optimal CAR T cells transduced with this CAR elicited similar anti-MM cytotoxic response like the original CAR028, but without having significant off-tumor toxicity on primary hematopoietic cells. Furthermore their long-term proliferation capacity was also similar to the original high affinity CAR028 T cells and they maintained Th1 cytokine production, which was even better than the other potential candidate CARB1.

To our knowledge this is the first study where CARs bearing scFvs with different antigen affinities are thoroughly tested *in vitro* and scored for all the above-mentioned properties, which define the immunotherapeutic potency of CAR T cells. Importantly, the capacity of CD38-CARA4 T cells to

delay MM tumor growth in a manner similar high affinity CD38-CAR028 T cells was also confirmed in an *in vivo* murine xenograft model.

To date, most studies investigating the on-target off-tumor effects of CAR T cell therapy make the use of artificial modeling for "healthy cells" using tumor cell lines which express or are transduced to express the target antigen in low levels.[15,16,35] Although valuable in several aspects, such an approach is not ideal for evaluating the off-tumor effects of CAR T cells, since several other differences between tumor and healthy cells, especially the differences in susceptibility to cytolysis, are neglected. Therefore in our approach we always compared primary tumor cells with primary healthy cells, whose relative low proliferation rate may render them more susceptible to cytotoxicity. Moreover, in order to reduce variability and to simulate the *in vivo* clinical setting as good as possible, we executed all our *in vitro* testing of tumor cells and the healthy cells side by side, in the same compartment (BM) and at the same time. As it is suggested that results from *in vivo* models are more relevant for the potential toxicity of CAR T cell treatment,[34] we also used primary human hematopoietic progenitor cells in our *in vivo* assays. In this model, $CD34^+$ hematopoietic progenitor cells, which were inoculated in a humanized xenografted environment[13,29,36] were detectable up to three weeks in all treatment groups. This three-week evaluation period was sufficient since in the same time frame we also detected the highest level of anti-MM reactivity. Neither the high affinity CAR T cells nor the optimized affinity CAR T cells disturbed the FLI signal from the inoculated CD34 progenitor cells. However, further analyses revealed that the maintenance of the $CD38^+$ progenitor compartment was achieved only in mice treated with the low affinity CARA4, confirming the low reactivity of our lead candidate towards healthy $CD38^+$ cells.

Finally, while we have been able to optimize the antigen recognition affinity of CARs, we think that these CARs need further evaluation with respect to their signaling requirements as we have tested only CARs with a 4-1BB co-stimulatory domain. It has recently been shown that that differences in the CAR configuration, either harboring CD28 or 4-1BB co-stimulatory domains, has a large effect on the killing capacity or persistence of CAR T cells.[25,37–40] In order to retain a certain pressure on tumor cells, the co-stimulatory domains can shape the activation status of CAR T cells, as well as subsequent

proliferation and cytokine production.[25,37,41] Accordingly, patient relapses seen in CAR-trials can be caused due to the poor longevity and persistence of CAR T cells. The differentiation status of the CAR T cells (central memory, effector memory or effectors) can somehow predict the *in vivo* longevity of the CAR T cells. Interestingly, in contrast to previous studies,[14–16,34] where no difference in immunophenotype was observed when lowering the affinity of CARs, we found the maintenance of $CD38^+$ CAR T cells when using the lower affinity CARs (Supplemental Fig. S3). Furthermore, we observed an apparent higher percentage of naïve and central memory cells in lower affinity CD38-CAR T cells compared to the original CAR028 T cells at the end of production stage, after which the CART cells are generally injected *in vivo*. Nonetheless, all cells eventually converted to the effector memory phenotype after prolonged *in vitro* culture, suggesting that the use of other co-stimulatory domains could reveal more optimal designs for low affinity CARs.

In conclusion, our data support the feasibility of the light chain exchange method as a new approach to generate a large panel of scFvs with a wide range of affinities for a TAA epitope. We, here, propose a stepwise rational *in vitro* and *in vivo* assessment and scoring of lower affinity CAR T cells in order to identify candidates with a strong tumoricidal function and minimal off-tumor toxicity. In addition to scFv affinity, future studies should include other aspects of the CAR design such as the costimulatory moieties and the targeting of different epitopes in order to achieve optimal selective CAR T cell functionality.

Acknowledgements: The authors thank Michel Sadelain (MSKCC) for providing the retroviral construct SFG with 4-1BB-CD3ζ–LNGFR transgene. The RAG2$^{-/-}$γc$^{-/-}$ mice used in this study were originally obtained from the Amsterdam Medical Center (AMC, Amsterdam, The Netherlands). We also thank Patrick Celie from the NKI Protein Facility for cloning, expression and purification of recombinant CD38 protein and to Genmab Utrecht for technical and infrastructure assistance in the production and testing of new antibodies with the light chain exchange technology. This work is in part executed by the financial support of 'Fonds Stimulans' the Netherlands (E.D. and T.M) and the European Commission (Marie Curie Individual Fellowship to M.T.)

Conflict of interest disclosure: T.M., H.M.L. and N.W.C.J.D. received project grant support from Genmab, Janssen and Celgene.

Author contribution: Conceptualization, E.D., M.T., R.W.J.G., H.M.L. and T.M.; Investigation, E.D., M.T., R.P., R.J.K.; Formal analysis, E.D. M.T. and T.M.; Resources, A.C.M.M., R.W.J.G., H.Y. and J.B.; Writing – Original Draft, E.D., M.T. and T.M.; Writing – Review & Editing, E.D., M.T., R.P., A.C.M.M., R.W.J.G., S.Z., N.W.C.J.D., H.M.L. and T.M.; Funding Acquisition, H.M.L. and T.M.; Supervision, M.T., S.Z., N.W.C.J.D., R.W.J.G., H.M.L. and T.M

References

1. Porter, DL, Levine, BL, Kalos, M, Bagg, A and June, CH (2011). Chimeric antigen receptor-modified T cells in chronic lymphoid leukemia. N. Engl. J. Med. **365**: 725–733.
2. Grupp, SA, Kalos, M, Barrett, D, Aplenc, R, Porter, DL, Rheingold, SR, et al. (2013). Chimeric Antigen Receptor–Modified T Cells for Acute Lymphoid Leukemia. N. Engl. J. Med. **368**: 1509–1518.
3. Maude, SL, Frey, N, Shaw, P a., Aplenc, R, Barrett, DM, Bunin, NJ, et al. (2014). Chimeric Antigen Receptor T Cells for Sustained Remissions in Leukemia. N. Engl. J. Med. **371**: 1507–1517.
4. Brentjens, RJ, Rivière, I, Park, JH, Davila, ML, Wang, X, Stefanski, J, et al. (2011). Safety and persistence of adoptively transferred autologous CD19-targeted T cells in patients with relapsed or chemotherapy refractory B-cell leukemias. Blood **118**: 4817–4828.
5. Kochenderfer, JN, Dudley, ME, Feldman, S a, Wilson, WH, Spaner, DE, Maric, I, et al. (2012). B-cell depletion and remissions of malignancy along with cytokine-associated toxicity in a clinical trial of anti-CD19 chimeric-antigen-receptor-transduced T cells. Blood **119**: 2709–2720.
6. Cheever, MA, Allison, JP, Ferris, AS, Finn, OJ, Hastings, BM, Hecht, TT, et al. (2009). The prioritization of cancer antigens: a national cancer institute pilot project for the acceleration of translational research. Clin. Cancer Res. **15**: 5323–5337.
7. Sadelain, M, Brentjens, R and Rivière, I (2013). The basic principles of chimeric antigen receptor design. Cancer Discov. **3**: 388–398.
8. Lamers, CHJ, Sleijfer, S, Vulto, AG, Kruit, WHJ, Kliffen, M, Debets, R, et al. (2006). Treatment of metastatic renal cell carcinoma with autologous T-lymphocytes genetically retargeted against carbonic anhydrase IX: first clinical experience. J. Clin. Oncol. **24**: 904–912.
9. Parkhurst, MR, Yang, JC, Langan, RC, Dudley, ME, Nathan, D-AN, Feldman, SA, et al. (2011). T cells targeting carcinoembryonic antigen can mediate regression of metastatic colorectal cancer but induce severe transient colitis. Mol. Ther. **19**: 620–626.
10. Davila, ML, Riviere, I, Wang, X, Bartido, S, Park, J, Curran, K, et al. (2014). Efficacy and toxicity management of 19-28z CAR T cell therapy in B cell acute lymphoblastic leukemia. Sci. Transl. Med. **6**: 224–225.
11. Lee, DW, Kochenderfer, JN, Stetler-Stevenson, M, Cui, YK, Delbrook, C, Feldman, SA, et al. (2014). T cells expressing CD19 chimeric antigen receptors for acute lymphoblastic leukaemia in children and young adults: a phase 1 dose-escalation trial. Lancet **385**: 517–528.
12. Morgan, R a, Yang, JC, Kitano, M, Dudley, ME, Laurencot, CM and Rosenberg, S a (2010). Case report of a serious adverse event following the administration of T cells transduced with a chimeric antigen receptor recognizing ERBB2. Mol. Ther. **18**: 843–851.

13. Drent, E, Groen, RWJ, Noort, WA, Themeli, M, Lammerts van Bueren, JJ, Parren, PWHI, et al. (2016). Pre-clinical evaluation of CD38 chimeric antigen receptor engineered T cells for the treatment of multiple myeloma. Haematologica **101**: 616–625.
14. Hudecek, M, Lupo-Stanghellini, M-T, Kosasih, PL, Sommermeyer, D, Jensen, MC, Rader, C, et al. (2013). Receptor affinity and extracellular domain modifications affect tumor recognition by ROR1-specific chimeric antigen receptor T cells. Clin. Cancer Res. **19**: 3153–3164.
15. Caruso, HG, Hurton, L V., Najjar, A, Rushworth, D, Ang, S, Olivares, S, et al. (2015). Tuning Sensitivity of CAR to EGFR Density Limits Recognition of Normal Tissue While Maintaining Potent Antitumor Activity. Cancer Res. **75**: 3505–3518.
16. Liu, X, Jiang, S, Fang, C, Yang, S, Olalere, D, Pequignot, EC, et al. (2015). Affinity-Tuned ErbB2 or EGFR Chimeric Antigen Receptor T Cells Exhibit an Increased Therapeutic Index against Tumors in Mice. Cancer Res. **75**: 3596–3607.
17. Carter, P, Presta, L, Gorman, CM, Ridgway, JB, Henner, D, Wong, WL, et al. (1992). Humanization of an anti-p185HER2 antibody for human cancer therapy. Proc. Natl. Acad. Sci. U. S. A. **89**: 4285–4289.
18. Chmielewski, M, Hombach, A, Heuser, C, Adams, GP and Abken, H (2004). T cell activation by antibody-like immunoreceptors: increase in affinity of the single-chain fragment domain above threshold does not increase T cell activation against antigen-positive target cells but decreases selectivity. J. Immunol. **173**: 7647–7653.
19. Zhou, Y, Drummond, DC, Zou, H, Hayes, ME, Adams, GP, Kirpotin, DB, et al. (2007). Impact of Single-chain Fv Antibody Fragment Affinity on Nanoparticle Targeting of Epidermal Growth Factor Receptor-expressing Tumor Cells. J. Mol. Biol. **371**: 934–947.
20. Jayaram, N, Bhowmick, P and Martin, ACR (2012). Germline VH/VL pairing in antibodies. Protein Eng. Des. Sel. **25**: 523–529.
21. Yoshinaga, K, Matsumoto, M, Torikai, M, Sugyo, K, Kuroki, S, Nogami, K, et al. (2008). Ig L-chain Shuffling for Affinity Maturation of Phage Library-derived Human Anti-human MCP-1 Antibody Blocking its Chemotactic Activity. J. Biochem. **143**: 593–601.
22. Senn, BM, López-Macías, C, Kalinke, U, Lamarre, A, Isibasi, A, Zinkernagel, RM, et al. (2003). Combinatorial immunoglobulin light chain variability creates sufficient B cell diversity to mount protective antibody responses against pathogen infections. Eur. J. Immunol. **33**: 950–961.
23. Wardemann, H, Hammersen, J and Nussenzweig, MC (2004). Human autoantibody silencing by immunoglobulin light chains. J. Exp. Med. **200**: 191–199.
24. Vink, T, Oudshoorn-Dickmann, M, Roza, M, Reitsma, J-J and de Jong, RN (2014). A simple, robust and highly efficient transient expression system for producing antibodies. Methods **65**: 5–10.
25. Zhao, Z, Condomines, M, van der Stegen, SJC, Perna, F, Kloss, CC, Gunset, G, et al. (2015).

Structural Design of Engineered Costimulation Determines Tumor Rejection Kinetics and Persistence of CAR T Cells. Cancer Cell **28**: 415–428.

26. Kim, JH, Lee, S-R, Li, L-H, Park, H-J, Park, J-H, Lee, KY, et al. (2011). High Cleavage Efficiency of a 2A Peptide Derived from Porcine Teschovirus-1 in Human Cell Lines, Zebrafish and Mice. In: Thiel, V (ed.). PLoS One **6**: e18556.
27. Luna-Vargas, MPA, Christodoulou, E, Alfieri, A, van Dijk, WJ, Stadnik, M, Hibbert, RG, et al. (2011). Enabling high-throughput ligation-independent cloning and protein expression for the family of ubiquitin specific proteases. J. Struct. Biol. **175**: 113–119.
28. Sari, D, Gupta, K, Thimiri Govinda Raj, DB, Aubert, A, Drncová, P, Garzoni, F, et al. (2016). The MultiBac Baculovirus/Insect Cell Expression Vector System for Producing Complex Protein Biologics. Adv. Exp. Med. Biol. **896**: 199–215.
29. Groen, RWJ, Noort, W a, Raymakers, RA, Prins, H-JJ, Aalders, L, Hofhuis, FM, et al. (2012). Reconstructing the human hematopoietic niche in immunodeficient mice: Opportunities for studying primary multiple myeloma. Blood **120**: 9–16.
30. Bostrom, J, Yu, S-F, Kan, D, Appleton, BA, Lee, C V., Billeci, K, et al. (2009). Variants of the Antibody Herceptin That Interact with HER2 and VEGF at the Antigen Binding Site. Science (80-.). **323**: 1610–1614.
31. Lamdan, H, Gavilondo, J V, Muñoz, Y, Pupo, A, Huerta, V, Musacchio, A, et al. (2013). Affinity maturation and fine functional mapping of an antibody fragment against a novel neutralizing epitope on human vascular endothelial growth factor. Mol. BioSyst. Mol. BioSyst **9**: 2097–2106.
32. Raposo, B, Dobritzsch, D, Ge, C, Ekman, D, Xu, B, Lindh, I, et al. (2014). Epitope-specific antibody response is controlled by immunoglobulin V(H) polymorphisms. J. Exp. Med. **211**: 405–411.
33. Ramos, CA, Savoldo, B and Dotti, G (2014). CD19-CAR trials. Cancer J. **20**: 112–118.
34. Johnson, LA, Scholler, J, Ohkuri, T, Kosaka, A, Patel, PR, McGettigan, SE, et al. (2015). Rational development and characterization of humanized anti-EGFR variant III chimeric antigen receptor T cells for glioblastoma. Sci. Transl. Med. **7**: 275ra22.
35. Morsut, L, Roybal, KT, Xiong, X, Gordley, RM, Coyle, SM, Thomson, M, et al. (2016). Engineering Customized Cell Sensing and Response Behaviors Using Synthetic Notch Receptors. Cell **164**: 780–791.
36. de Haart, SJ, van de Donk, NWCJ, Minnema, MC, Huang, JH, Aarts-Riemens, T, Bovenschen, N, et al. (2013). Accessory cells of the microenvironment protect multiple myeloma from T-cell cytotoxicity through cell adhesion-mediated immune resistance. Clin. Cancer Res. **19**: 5591–5601.
37. Abken, H (2016). Costimulation Engages the Gear in Driving CARs. Immunity **44**: 214–216.
38. Milone, MC, Fish, JD, Carpenito, C, Carroll, RG, Binder, GK, Teachey, D, et al. (2009).

Chimeric receptors containing CD137 signal transduction domains mediate enhanced survival of T cells and increased antileukemic efficacy in vivo. Mol. Ther. **17**: 1453–1464.

39. Kowolik, CM, Topp, MS, Gonzalez, S, Pfeiffer, T, Olivares, S, Gonzalez, N, et al. (2006). CD28 costimulation provided through a CD19-specific chimeric antigen receptor enhances in vivo persistence and antitumor efficacy of adoptively transferred T cells. Cancer Res. **66**: 10995–11004.

40. Cherkassky, L, Morello, A, Villena-Vargas, J, Feng, Y, Dimitrov, DS, Jones, DR, et al. (2016). Human CAR T cells with cell-intrinsic PD-1 checkpoint blockade resist tumor-mediated inhibition. J. Clin. Invest. **126**: 3130–3144.

41. van der Stegen, SJC, Hamieh, M and Sadelain, M (2015). The pharmacology of second-generation chimeric antigen receptors. Nat. Rev. Drug Discov. **14**: 499–509.

Figure legends

Figure 1 Selection of low affinity CD38 antibodies. (A) Schematic cartoon of light chain exchange method and overview of antibody generation and selection process. (B) Representative graphs of binding assays performed with CHO cells transfected with CD38 (CHO-CD38) or wildtype (WT). His-CD38 are beads coated with recombinant CD38 and detected with IgG or Fab fragments with fluorchrome beads. Rows indicate wildtype (WT 028) antibody 028 and class A, B and C, as defined by A= positive binding in all assays, B= positive in the cell binding and IgG, C= only positive binding on CHO-CD38. (C) Quantified EC50 values (mg/ml) of different binding assays. (D) Molecule association and dissociation curves. Interferometric profile shifts are measured and its magnitude is plotted as a function of time. (E) Interferometric profiles of the antibodies are quantified into K_D values (M), on and off-rates (Kon (1/Ms) and Koff (1/s)). N=2 +/- SD.

Figure 2 Lytic capacity of different affinity CD38-CAR T cells. Lysis of cell line UM9 by different affinity CD38-CAR T cells when co-incubated with luciferase-transduced MM cell line UM9 for a 16 hours, cytotoxicity was measured with BLI, n=2. Graphs are divided in three affinity subcategories. Class A CARs are derived from class A antibodies, with the highest affinity, to class C with the lowest affinity. CARs with the 028 variable heavy chain (VH) are numbered 1-4 in each class and CARs with 024 VH 5-8.

Figure 3 Phenotypic profiles of lower affinity CD38-CAR T cells. (A) 24 hours after co-incubation with $CD38^+$ target cell line UM9 or $CD38^-$ target U266, E:T ratio 1:1, cytokine secretion by mock or CD38-CAR028, A1, A4, B1 or B3 T cells was measured with a flow cytometry-based assay in the cell free supernatants. Graph shows the secretion of IFN-γ, TNF and IL-2. n=2, mean +/- SEM, * indicates p value <0.05 and ** <0.01 using one-way analysis of variance and subsequent multiple comparison. (B) CD38-CAR T cells were stimulated with MM target UM9 E:T ratio 1:3 one week after transduced and followed weekly. Cells were counted and % of CAR^+ cells were determined by flow cytometry. Figure indicated growth of CAR^+ cells in the culture. (●) indicate mock and open squares (□)

indicate CD38-CAR028, (▲) CARA1, (◆) CARA4, (▼) CARB1, (●) CARB3. N=2 mean +/- SEM, ns=not significant (C) Phenotypic profile of each CD38-CAR T cell type was determined before (week 0) and after (week 1) expansion with markers CD45RA and CD62L. Percentage of total of cells is depicted naive (CD45RA+/CD62L+) central memory (CM) (CD45RA-/CD62L+), effector memory (EM) ($CD45RA^-/CD62L^-$). N=2 mean +/- SEM, ns=not significant. Statistical analysis was done using one-way analysis of variance and subsequent multiple comparison.

Figure 4 Lytic capacity of lower affinity CD38-CAR T cells towards Multiple Myeloma bone marrow. Bone marrow (BM-MNCs) samples of four MM patients with 20-40% MM cells were co-incubated, mock or CD38-CAR028, A1, A4, B1 or B3 T cells for 16 h. The graphs depict the resulting lysis of (A) $CD138^+/CD38^+$ cells (MM) (B) $CD38^+$ MNCs (non-MM) and (C) total MNCs in E:T (E:BM-MNC) ratio 1:1. Representative figure of other ratios in supplemental Fig. S5. (●) indicate mock and open squares (□) indicate CD38-CAR028, (▲) CARA1, (◆) CARA4, (▼) CARB1, (⬣) CARB3. The % lysis in these flow cytometry assays was calculated as described in the methods section. N=4, median +/- range, * indicates p value <0.05 and ** <0.01 using Kruskal-Wallis analysis of variance and subsequent Mann-Whitney comparison. (D) Flow cytometry dot plots depicting MM-BM with $CD138^+/CD38^{++}$ cells (MM), and $CD138^-/CD38^+$ healthy cells. The CD38 threshold for lysis is indicated with 2 horizontal bars on voltage 10^3 (threshold for high affinity CD38-CAR028) and 10^4 for some of the lower affinity CD38-CARs.

Figure 5 CARA4 is the best candidate for a lower affinity CAR. Peripheral blood mononuclear cells (PBMCs) of a healthy donor were co-incubated with mock, high affinity CD38-CAR028 or low affinity CD38-CARA4 T cells for 16 h. The graphs depict the resulting lysis of $CD3^+$ (T cells), $CD56^+$ (NK cells) or $CD19^+$ (B cells), their total or $CD38^+$ fraction. Circles (●) indicate mock and open squares (□) indicate CD38-CAR028, triangle (▲) CARA1 and diamond (◆) CARA4. The % lysis in these flow cytometry assays was calculated as described in the methods section.

Figure 6 High and low affinity CD38-CAR T cells are similarly effective *in vivo*. Mice were i.v. injected with $10x10^6$ cells of tumor cell line UM9 and treated one week after with i.v. injections of 5 x 10^6 mock, high affinity CD38-CAR028 or low affinity CD38-CARA4 T cells. (A) Bioluminescence images (BLI) are shown per group of each week. (B) Analysis of tumor load in mice by quantification of BLI measurements. Each group contained four mice, each harboring 4 scaffolds. Closed circles (●) indicate mock and open squares (□) indicate CD38-CAR028 and (◆) CD38-CARA4. N=4, Results are median tumor load (cpm/cm^2) of 4 mice +/- range, * indicates p value <0.05, ** <0.01 and *** <0.001 using Kruskal-Wallis analysis of variance.

Figure 7 High affinity CD38-CAR T cells affect CD34 hematopoietic progenitor cells. (A) Mice were intrascaffold injected with 1 x 10^6 fluorescently (FarRed) labeled CD34$^+$ and treated one week after with i.v. injections of 5 x 10^6 mock, high affinity CD38-CAR028 or low affinity CD38-CARA4 T cells. (A) Fluorescence images (FLI) are shown per group at week 1 and 3. (B) Percentages of CD34$^{+/-}$ and CD38$^{+/-}$ cells in the total population of FarRed$^+$ cells, that were present in the scaffold in post-mortem tissue samples analyzed by flow cytometry. Results % CD34$^{+/-}$ and CD38$^{+/-}$ of four mice per group, two scaffold per mouse +/- range, * indicates p value <0.05, using Mann-Whitney test on CD38$^+$ percentages. (C) Total number of manually counted cells were adjusted using the percentage of FarRed$^+$ cells as measured by flow cytometry and the percentage of CD34$^{+/-}$ and CD38$^{+/-}$ in B. N=4 mice per group, median +/- range.

Figure 1

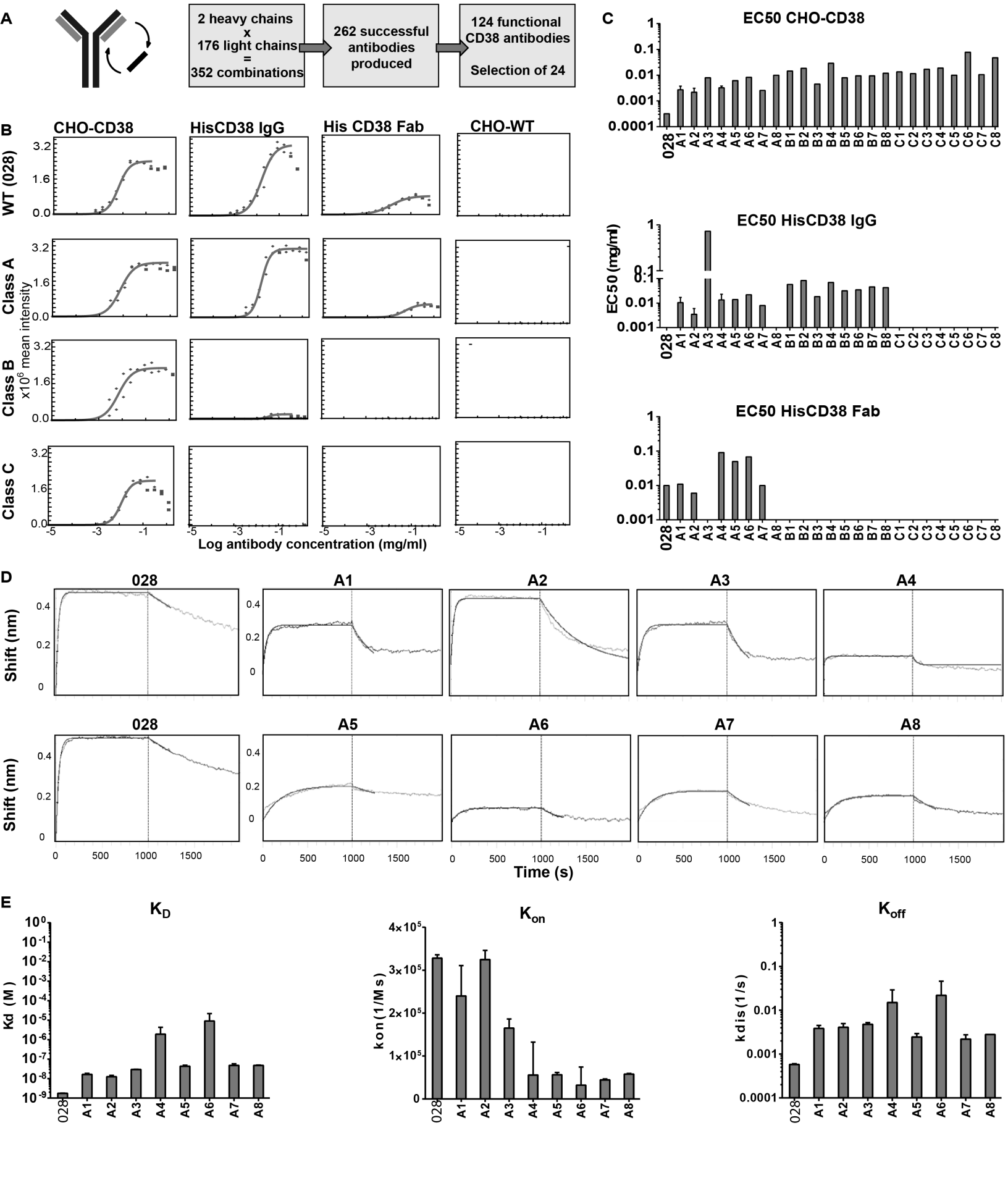
A
2 heavy chains x 176 light chains = 352 combinations
262 successful antibodies produced
124 functional CD38 antibodies
Selection of 24
B
CHO-CD38
HisCD38 IgG
His CD38 Fab
CHO-WT
WT (028)
Class A
Class B
Class C
x10^6 mean intensity
Log antibody concentration (mg/ml)
C
EC50 CHO-CD38
EC50 HisCD38 IgG
EC50 (mg/ml)
EC50 HisCD38 Fab
028 A1 A2 A3 A4 A5 A6 A7 A8 B1 B2 B3 B4 B5 B6 B7 B8 C1 C2 C3 C4 C5 C6 C7 C8
D
028
A1
A2
A3
A4
A5
A6
A7
A8
Shift (nm)
Time (s)
E
K_D
K_on
K_off
Kd (M)
kon(1/Ms)
kdis(1/s)

Figure 2

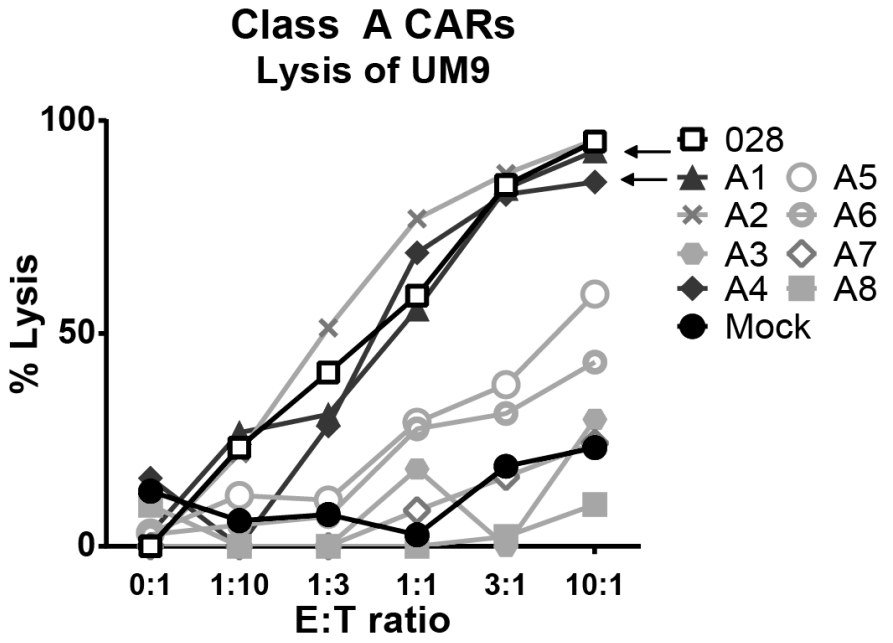
Class A CARs
Lysis of UM9
100
50
0
% Lysis
0:1
1:10
1:3
1:1
3:1
10:1
E:T ratio
028
A1
A2
A3
A4
A5
A6
A7
A8
Mock

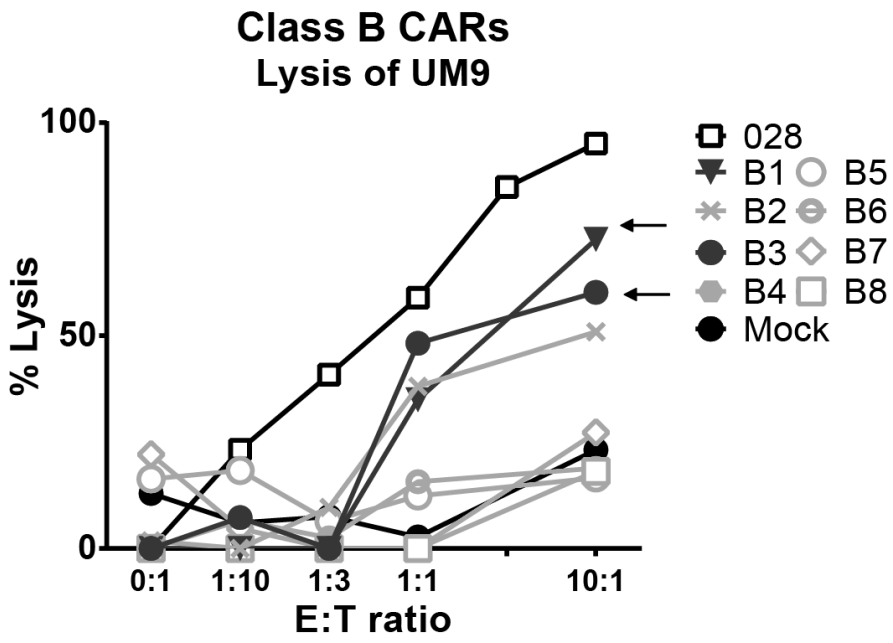
Class B CARs
Lysis of UM9
100
50
0
% Lysis
0:1
1:10
1:3
1:1
10:1
E:T ratio
028
B1
B2
B3
B4
B5
B6
B7
B8
Mock

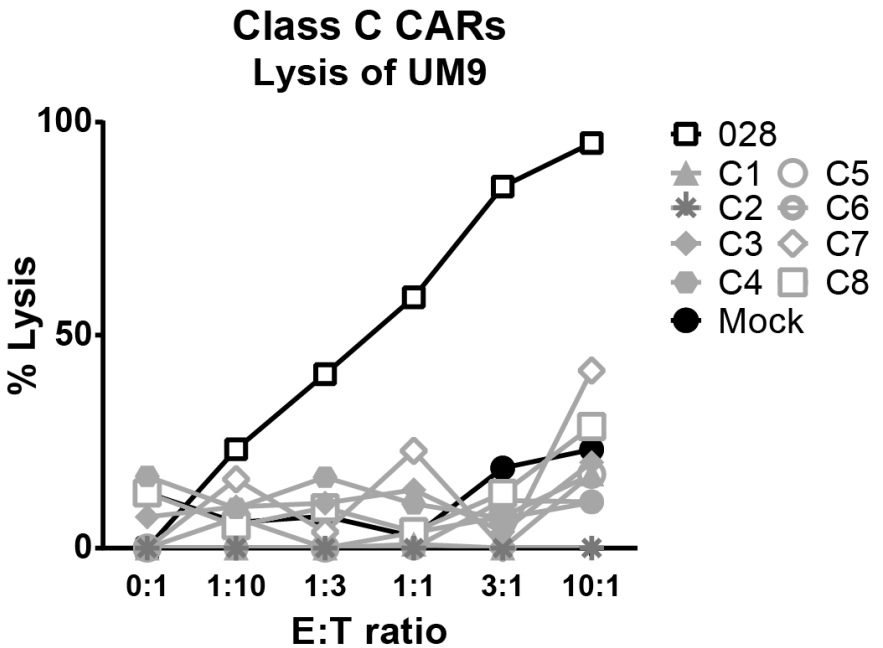
Class C CARs
Lysis of UM9
100
50
0
% Lysis
0:1
1:10
1:3
1:1
3:1
10:1
E:T ratio
028
C1
C2
C3
C4
C5
C6
C7
C8
Mock

Figure 3

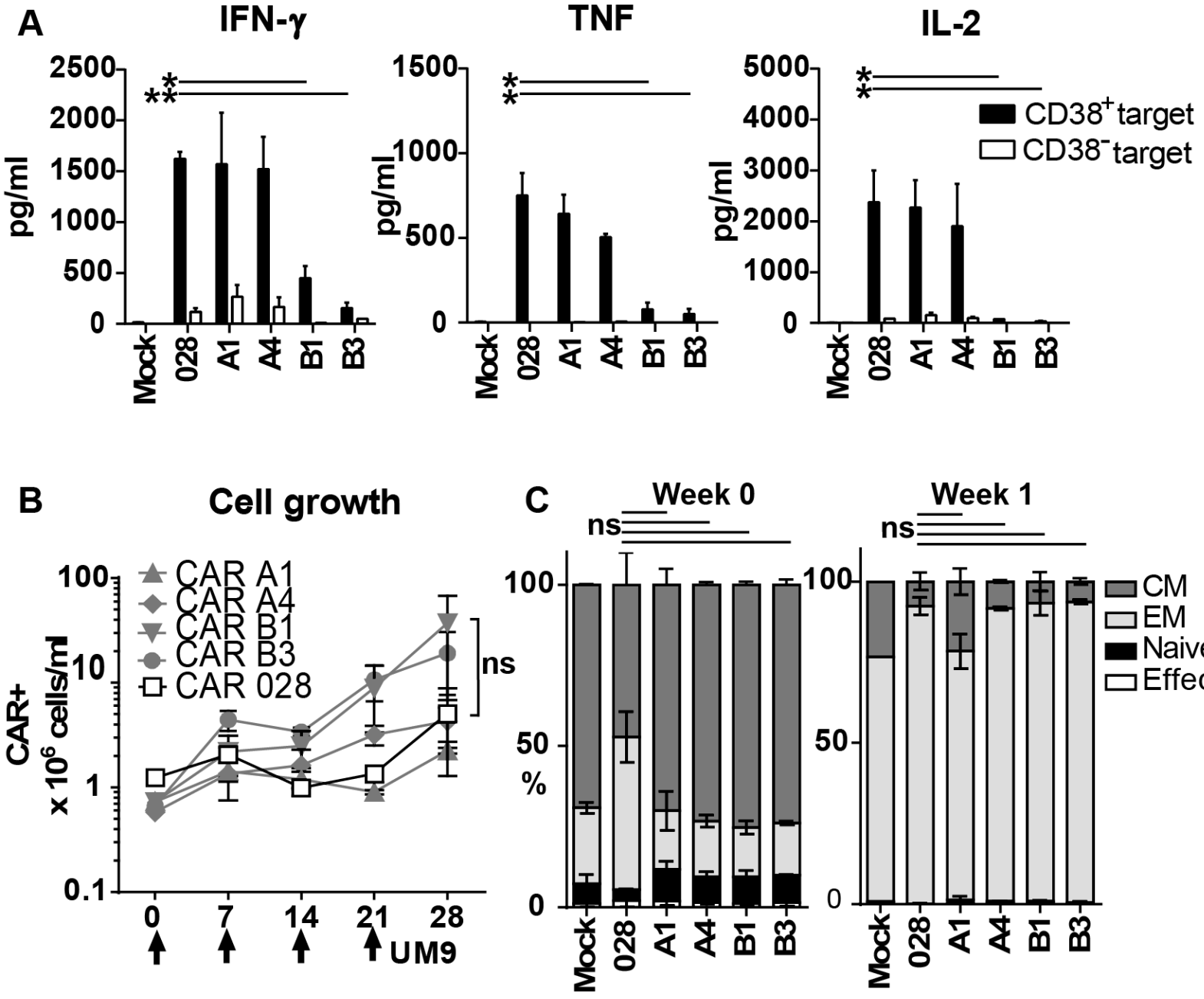
A
IFN-γ
TNF
IL-2
pg/ml
2500
2000
1500
1000
500
0
**
**
Mock
028
A1
A4
B1
B3
CD38+target
CD38-target
B
Cell growth
CAR A1
CAR A4
CAR B1
CAR B3
CAR 028
CAR+
x 10^6 cells/ml
100
10
1
0.1
ns
0
7
14
21
28
UM9
C
Week 0
Week 1
ns
%
50
CM
EM
Naive
Effector

Figure 4

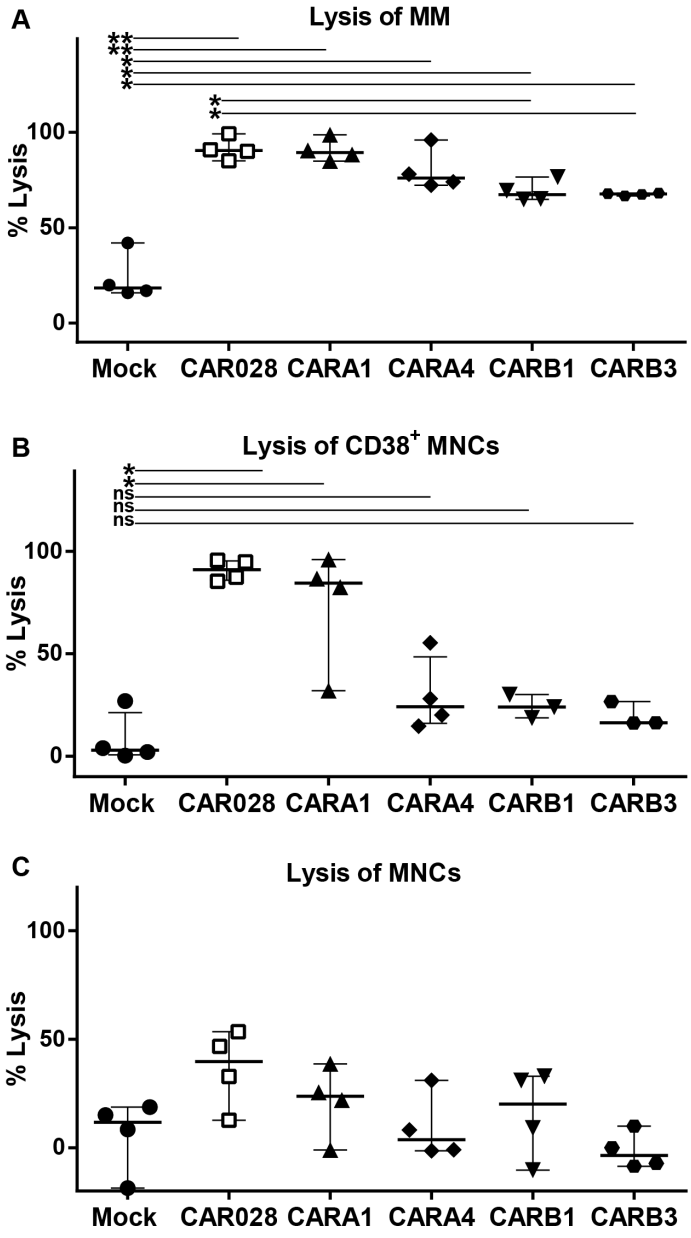
A
Lysis of MM
% Lysis
100
50
0
Mock
CAR028
CARA1
CARA4
CARB1
CARB3
B
Lysis of CD38+ MNCs
% Lysis
ns
C
Lysis of MNCs
% Lysis

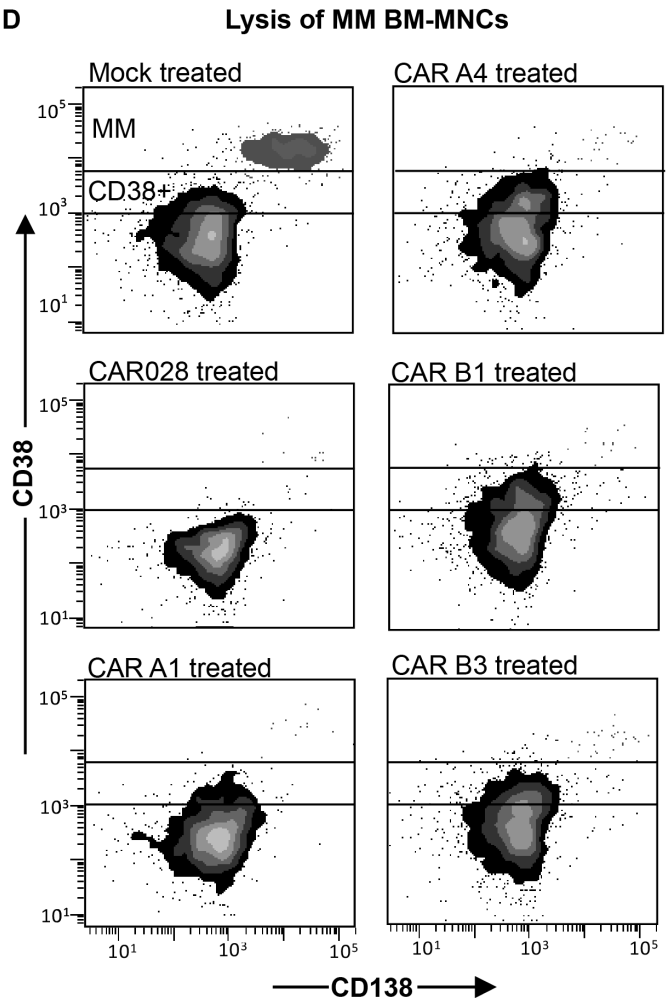
D
Lysis of MM BM-MNCs
Mock treated
CAR A4 treated
MM
CD38+
CAR028 treated
CAR B1 treated
CAR A1 treated
CAR B3 treated
CD38
CD138

Figure 5

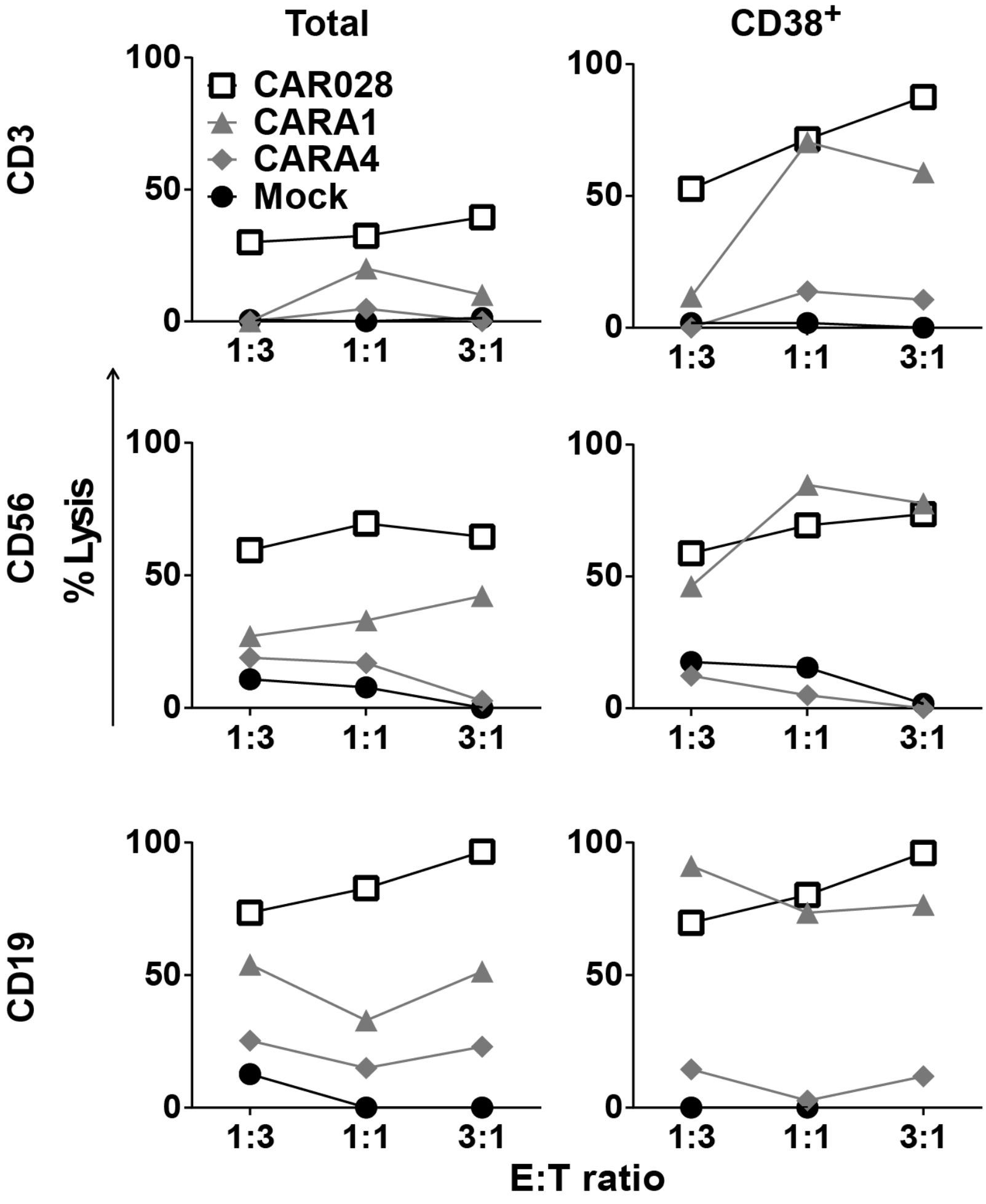
Total
CD38+
CAR028
CARA1
CARA4
Mock
CD3
CD56
CD19
% Lysis
100
50
0
1:3
1:1
3:1
E:T ratio

Figure 6

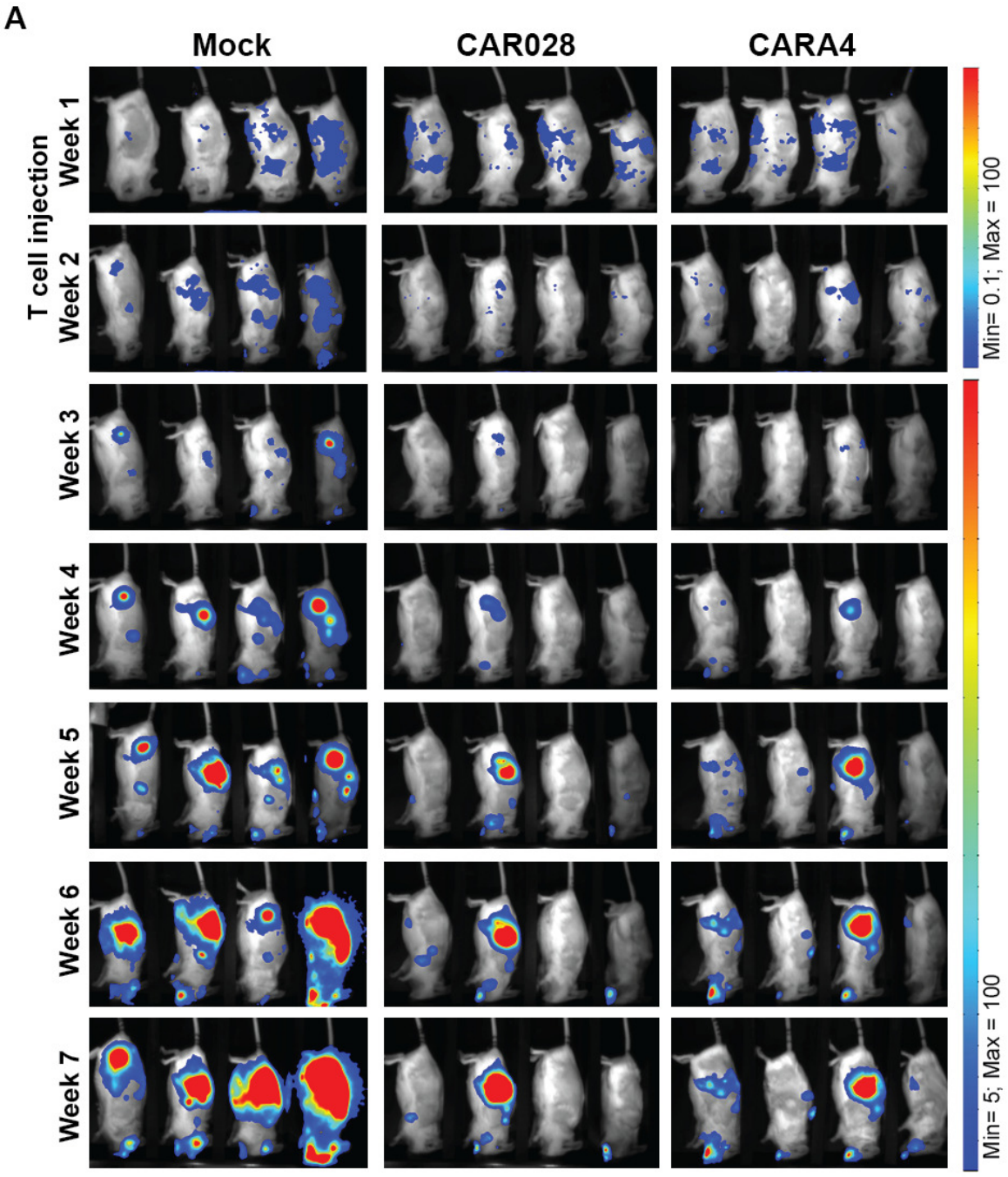
A
Mock
CAR028
CARA4
T cell injection
Week 1
Week 2
Week 3
Week 4
Week 5
Week 6
Week 7
Min= 0.1; Max = 100
Min= 5; Max = 100

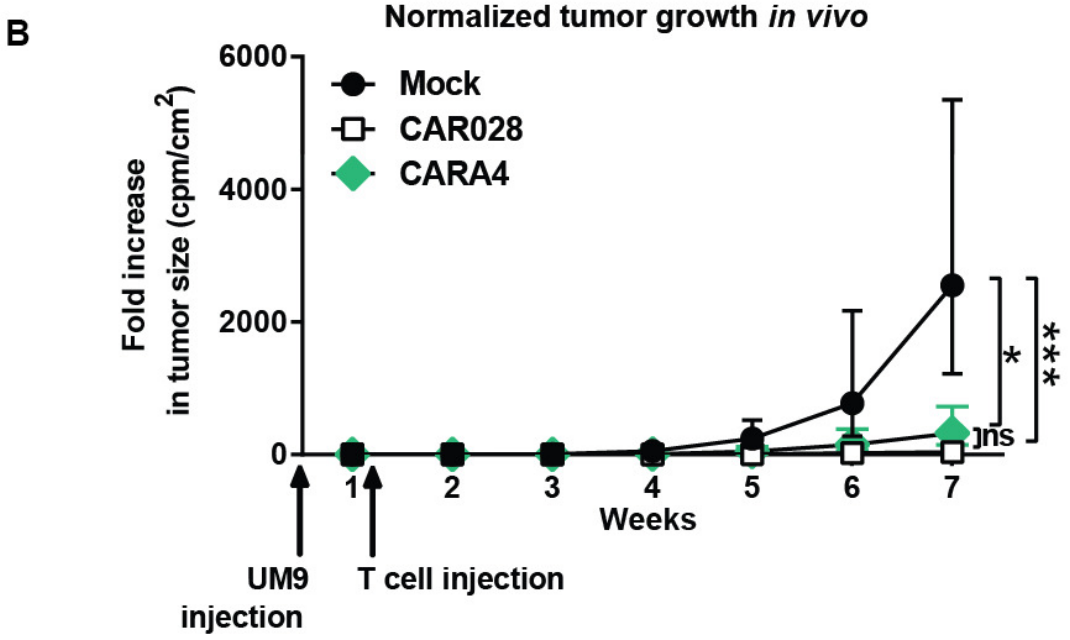
B
Normalized tumor growth *in vivo*
Fold increase in tumor size (cpm/cm^2)
6000
4000
2000
0
Mock
CAR028
CARA4
1
2
3
4
5
6
7
Weeks
*
***
ns
UM9 injection
T cell injection

Figure 7

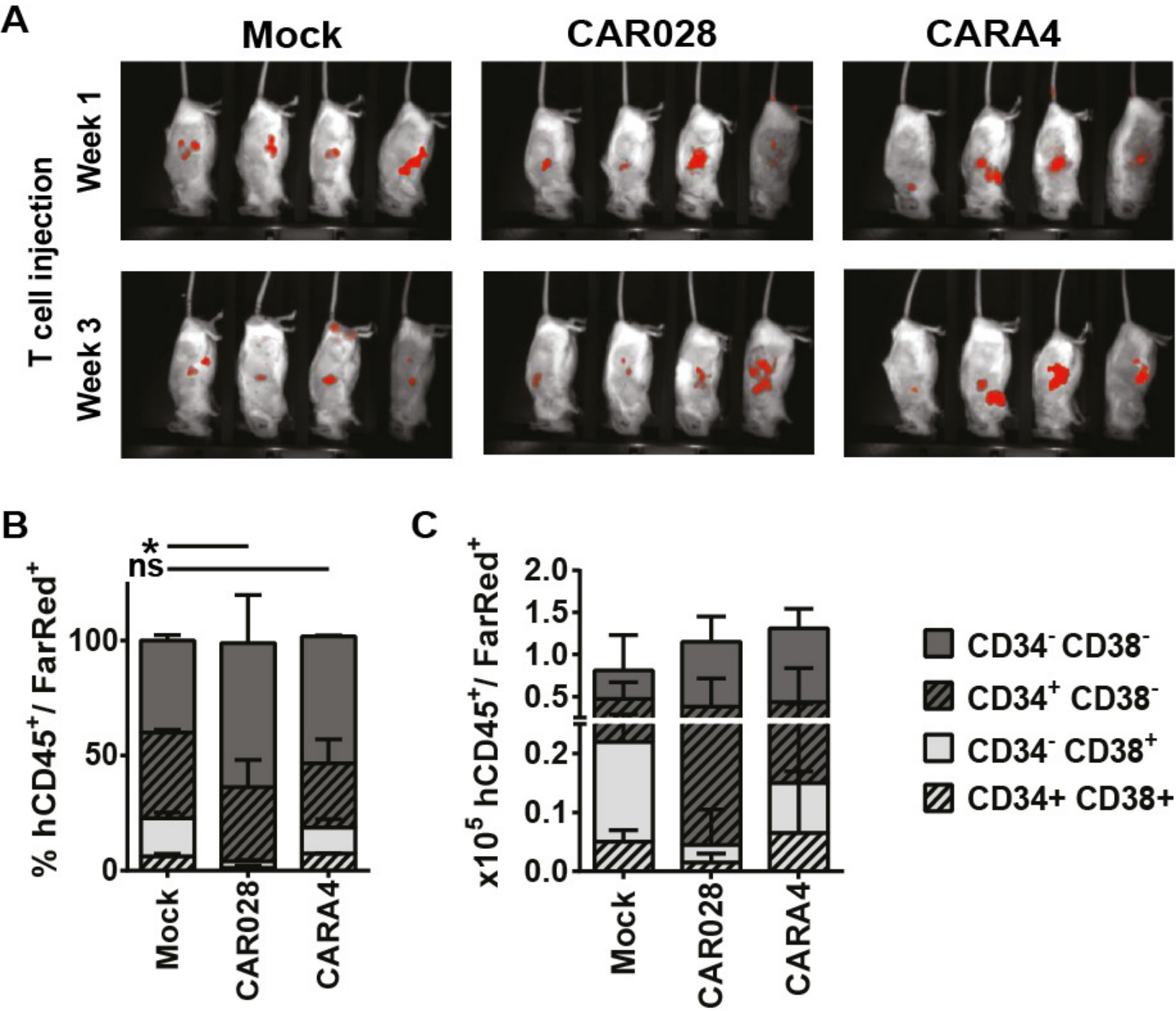
A
Mock
CAR028
CARA4
T cell injection
Week 1
Week 3
B
% hCD45+/ FarRed+
*
ns
100
50
0
Mock
CAR028
CARA4
C
x10^5 hCD45+/ FarRed+
2.0
1.5
1.0
0.5
0.2
0.1
0.0
Mock
CAR028
CARA4
CD34- CD38-
CD34+ CD38-
CD34- CD38+
CD34+ CD38+